Impact Ionization Coefficients in $(Al_xGa_{1-x})_{0.52}In_{0.48}P$ and $Al_xGa_{1-x}As$ Lattice-Matched to GaAs

Harry I. J. Lewis, Liang Qiao, Jeng Shiuh Cheong, Aina N. A. P. Baharuddin, Andrey B. Krysa, Beng Koon Ng, *Member, IEEE*, James E. Green, *Member, IEEE*, and John P. R. David, *Fellow, IEEE*

***Abstract*— The impact ionization characteristics of $(Al_xGa_{1-x})_{0.52}In_{0.48}P$ have been studied comprehensively across the full composition range. Electron and hole impact ionization coefficients (α and β, respectively) have been extracted from avalanche multiplication and excess noise data for seven different compositions and compared to those of $Al_xGa_{1-x}As$. While both α and β initially decrease gradually with increasing bandgap, a sharp decrease in β occurs in $(Al_xGa_{1-x})_{0.52}In_{0.48}P$ when $x > 0.61$, while α decreases only slightly. α and β decrease minimally with further increases in x and the breakdown voltage saturates. This behavior is broadly similar to that seen in $Al_xGa_{1-x}As$, suggesting that it may be related to the details of the conduction band structure as it becomes increasingly indirect in both alloy systems.**

***Index Terms*— AlGaAs, AlGaInP, avalanche breakdown, avalanche photodiodes (APDs), excess noise, GaAs, impact ionization.**

I. Introduction

IMPACT ionization is the mechanism of carrier generation in semiconductors that are responsible for the internal gain of avalanche photodiodes (APDs). It is also the cause of avalanche breakdown, which is a failure mechanism in many electronic devices that are subject to a high electric field. It is therefore important that the characterization of semiconductor materials includes accurate knowledge of the electron and hole impact ionization coefficients, referred to as α and β, respectively. These parameters are defined as the reciprocal of the mean distance that a carrier travels between ionization events at a given electric field.

Manuscript received April 8, 2021; revised May 17, 2021; accepted May 31, 2021. Date of publication June 24, 2021; date of current version July 23, 2021. This work was supported by the Engineering and Physical Sciences Research Council (EPSRC) under Grant EP/R513313/1. The review of this article was arranged by Editor G. Ghione. *(Corresponding author: John P. R. David.)*

Harry I. J. Lewis, Liang Qiao, Jeng Shiuh Cheong, Aina N. A. P. Baharuddin, Andrey B. Krysa, James E. Green, and John P. R. David are with the Department of Electronic and Electrical Engineering, University of Sheffield, Sheffield S1 3JD, U.K. (e-mail: j.p.david@sheffield.ac.uk).

Beng Koon Ng is with the School of Electrical and Electronic Engineering, Nanyang Technological University, Singapore 639798.

Color versions of one or more figures in this article are available at https://doi.org/10.1109/TED.2021.3086800.

Digital Object Identifier 10.1109/TED.2021.3086800

$(Al_xGa_{1-x})_{0.52}In_{0.48}P$ (AlGaInP hereafter) has a tunable wide bandgap of 1.8–2.2 eV, the largest of any material that can be grown lattice-matched to GaAs. To date, only the impact ionization characteristics of the ternary end points of AlInP [1] and GaInP [2] have been studied. The only other study of intermediate compositions looked at the avalanche breakdown voltages in a number of heterojunction diodes [3]. AlGaInP APDs exhibit negligible dark currents even at fields close to breakdown [4], and the excess noise factor in thin AlInP devices has been shown to be similar to that in silicon [5]. The wide bandgap of AlGaInP also results in minimal variation in breakdown voltage and dark currents with temperature [6], [7] and AlInP X-ray detectors with good high-temperature performance have been reported [8]. The dark currents and temperature dependence characteristics of AlInP and GaInP devices [6] compare favorably with recently reported GaN APDs grown on GaN substrates [9], but with the advantage of the low cost and mature technology associated with GaAs substrates. There is also interest in GaAs-based SAM-APDs with wide bandgap multiplication regions, using GaNAsSb and GaSb absorption regions for SWIR detection [10], [11]. The understanding gained from this alloy system may also be useful in determining the optimum compositions of other Al/Ga containing alloy systems such as $Al_xGa_{1-x}As_{0.56}Sb_{0.44}$, for which extremely low-noise APDs have been recently reported [12], [13].

This work reports experimentally determined impact ionization coefficients for seven different compositions of $(Al_xGa_{1-x})_{0.52}In_{0.48}P$, from $x = 0$ to $x = 1$, extracted from measurements of the avalanche multiplication and excess noise factor. The effects on the ionization coefficients of varying the aluminum concentration in this alloy are compared to the results seen in AlGaAs, a similar material system that can also be grown lattice-matched to GaAs.

II. Wafer and Device Details

A series of homojunction p^+-i-n^+ $(Al_xGa_{1-x})_{0.5}2In_{0.48}P$ wafers with $x = 0$, 0.31, 0.47, 0.61, 0.64, 0.78 and 1 were grown by atmospheric pressure Metal-Organic Chemical Vapour-Phase Epitaxy on 2” GaAs substrates, as previously

This work is licensed under a Creative Commons Attribution 4.0 License. For more information, see https://creativecommons.org/licenses/by/4.0/

TABLE I
PARAMETERS OF $(Al_xGa_{1-x})_{0.52}In_{0.48}P$ WAFERS USED IN THIS STUDY

Al fraction, x	Intrinsic region width, w [μm]	N_i [x10^{15}cm^{-3}] ± 1x10^{15}cm^{-3}	N_p [x10^{17}cm^{-3}] ± 1x10^{17}cm^{-3}
0	0.94	2	18
0.31	0.99	3.5	8
0.47	0.94	3	7.5
0.61	1.00	2	8
0.64	0.96	3.5	6
0.78	0.94	4.5	6
1	0.96	3	3.5

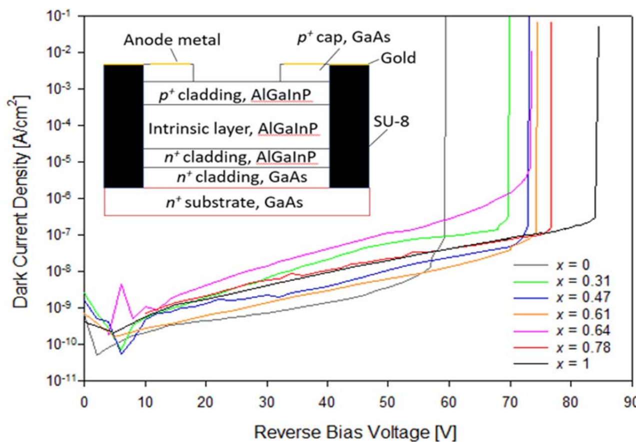

Fig. 1. Reverse bias dark current density for $(Al_xGa_{1-x})_{0.52}In_{0.48}P$ with different values of x. Inset is a schematic of the device structure.

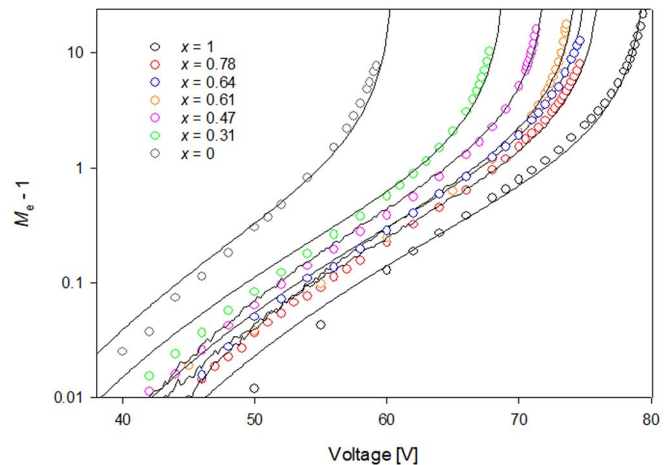

Fig. 2. Multiplication as a function of reverse bias for several compositions of $(Al_xGa_{1-x})_{0.52}In_{0.48}P$, in the form $M_e - 1$. Black lines show data simulated using the fitted ionization coefficients (the coefficients of Ong *et al.* [1] and Ghin *et al.* [2] were used to simulate data for AlInP and GaInP, respectively).

described in [14]. The parameters of these wafers are detailed in Table I. Each wafer had a nominal intrinsic region thickness, w, of 1 μm and p$^+$ and n$^+$ cladding layers of 1.0 and 0.3 μm, respectively. The wafers were capped with 50 nm thick p$^+$ GaAs, to ensure a good ohmic contact, and were grown on n$^+$ GaAs substrates. Circular mesa diode structures with optical windows were fabricated on these wafers using standard photolithography and wet chemical etching. Device radii were between 35 and 210 μm. The GaAs cap was removed by wet etching in the optical window regions. The mesa sidewalls were passivated with SU-8 and covered with gold to ensure that light could only enter the device through the top optical window as shown in the inset of Fig. 1. The depletion region widths and the doping densities of each layer were obtained using capacitance-voltage measurements. Dielectric constants were interpolated from those of GaP, InP, and AlP [15]–[17]. The thicknesses of the intrinsic regions in the devices were found to vary between 0.94 and 1.00 μm.

III. EXPERIMENTAL METHODS AND RESULTS

The dark currents for all samples were less than 1 nA at up to 95% of breakdown voltage (V_{bd}) as shown in Fig. 1 due to the wide bandgaps of these alloys. The exponential increase seen in the dark currents prior to V_{bd} is thought to be due mid-band traps in the material, which are known to occur in AlGaInP [18]. This means that the dark currents shown here are probably representative of defects in the specific wafers used in this study. Avalanche multiplication measurements were undertaken on these devices by measuring the change in photocurrent as a function of reverse bias. All data were for the case of pure electron initiated multiplication. This means that the avalanche multiplication process is initiated by electrons only rather than by both carrier types. The light sources used were a 430-nm LED for $x = 1$, a 460-nm LED for $x = 0.47$, 0.61, 0.64, and 0.78, and a 543-nm laser for $x = 0.31$ and $x = 0$.

The use of short wavelength light sources ensured that ≥99.9% of incident photons were absorbed in the p$^+$ top cladding layer of the devices, resulting in pure electron initiated photomultiplication. A longer wavelength was used for $x = 0$ and $x = 0.31$ due to the lower bandgap of these compositions. Using too short a wavelength results in a reduced photocurrent signal, as carrier recombination in the p$^+$ cladding reduces the number of carriers that diffuse into the depletion region. Phase-sensitive detection was used for photomultiplication measurements to separate the photocurrent from the dark currents and ensure accuracy. The multiplication (M_e) data is shown versus reverse bias voltage in Fig. 2. It is plotted in the form $M_e - 1$ on a log scale to show the onset of the impact ionization process at low bias. The threshold voltages at which the start of impact ionization can be measured and at which avalanche breakdown occurs increase with aluminum percentage. Due to the stochastic nature of the impact ionization process, the avalanche multiplication is accompanied by "excess noise" which increases with β/α ratio (k) for multiplication initiated by electrons [20]. Excess noise measurements were performed on these devices using the low-current noise measurement system of Qiao *et al.* [21], which is a modified version of the system of Lau *et al.* [22]. The results are shown in Fig. 3. Data for GaAs and $Al_xGa_{1-x}As$ ($x = 0.8$) are included for comparison as well as the McIntyre noise characteristics for different β/α ratios. The excess noise reduces in AlGaInP with

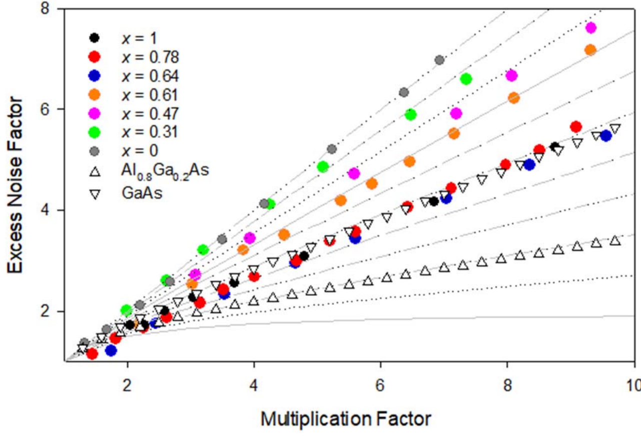

Fig. 3. Excess noise factor versus M_e for several compositions of $(Al_xGa_{1-x})_{0.52}In_{0.48}P$. The lines represent Macintyre's ideal noise curves for effective k values of 0 – 1, in steps of 0.1. Simulated data for comparable GaAs (Δ) and $Al_{0.8}Ga_{0.2}As$ (∇) structures are included for comparison [19].

increasing bandgap from k being approximately equal to 1 for $x = 0$ to approximately 0.5 for $x = 0.64$, after which it does not decrease further. We consider the slight differences in excess noise factor shown when $x \geq 0.64$ to be due to small differences in the normalization between wafer structures, and within experimental error. The largest relative decrease occurs between $x = 0.61$ and $x = 0.64$, despite only a small change in composition.

IV. Extraction of Ionization Coefficients

As only p-i-n structures were available for this study, it was not possible to obtain data for pure hole-initiated multiplication. From data for pure electron initiated multiplication, it was therefore necessary to use the excess noise data to determine the effective β/α ratio using Macintyre's equation for excess noise factor [20]

$$F = k_{\text{eff}} M + (2 - 1/M)(1 - k_{\text{eff}}) \tag{1}$$

where F is the excess noise factor, k_{eff} is the effective β/α ratio, and M is the multiplication factor. Knowledge of the β/α ratio then allows M_h to be inferred from the value of M_e. α and β can then be extracted from M_e and M_h, respectively [23]. In the case of ideal p-i-n structures, it is straightforward to use the equations in [23] analytically. However, the depletion region can extend significantly into the lower doped p-type cladding regions in these structures [14], particularly at higher biases. It was also necessary to account for the "dead space," the minimum distance that a carrier must travel before it acquires sufficient energy to ionize the lattice [24]. For the structures used in this study the effect of the dead space on the multiplication is small, but its effect on excess noise is nonnegligible. To account for all of these effects, the multiplication and noise data were simulated using the random path length (RPL) model of Cheong *et al.* [25]. This model uses an ionization probability density function to account for the dead space. It also accounts for any variation in the electric field profile across the device, to accurately simulate multiplication and excess noise. The ionization threshold energies, E_{the} and E_{thh}, for AlInP and GaInP are known [25], and those for the intermediate compositions were interpolated from these. The threshold energy for each intermediate composition was approximated as 2.05 times the energy bandgap, using bandgap values reported by Cheong *et al.* [14]. The values of the minimum energy bandgaps and threshold energies are given in Table II. In AlInP and GaInP, E_{the} and E_{thh} are the same, and this was assumed to be the case for the intermediate compositions. Simulated data were compared to the experimental data and optimized ionization coefficients were found using an iterative fitting method. The paramaterized ionization coefficients are represented by the following set of equations, where ξ represents electric field in V/cm, (2)–(5), as shown at the bottom of the page.

It should be noted that these parameterized coefficients should be used with an appropriate model where the effect of the threshold energy is included to accurately replicate experimental multiplication and excess noise. Ignoring the effect of the threshold energy and using a model where the

$$\alpha = (5.91\times10^6 - 1.12\times10^5 x - 6.05\times10^7 x^2 + 1.14\times10^8 x^3)\exp\left(\frac{-4.16x10^6 + 1.01x10^6 x - 1.63x10^6 x^2 - 3.58x10^6 x^3}{\xi}\right)\text{cm}^{-1} \tag{2}$$

$$\beta = (4.43\times10^6 + 4.98\times10^7 x - 2.12\times10^8 x^2 + 2.23\times10^8 x^3)\exp\left(\frac{-3.86\times10^6 - 5.71\times10^6 x + 1.99\times10^7 x^2 - 2.15\times10^7 x^3}{\xi}\right)\text{cm}^{-1}$$

for $x \leq 0.61$, and (3)

$$\alpha = (2.20\times10^8 - 8.42\times10^8 x + 1.09\times10^9 x^2 - 4.50\times10^8 x^3)\exp\left(\frac{8.26x10^6 - 4.68x10^7 x + 5.43x10^7 x^2 - 2.15x10^7 x^3}{\xi}\right)\text{cm}^{-1} \tag{4}$$

$$\beta = (8.88\times10^8 - 3.87\times10^9 x + 5.44\times10^9 x^2 - 2.39\times10^9 x^3)\exp\left(\frac{1.15x10^8 - 4.43x10^8 x + 5.35x10^8 x^2 - 2.14x10^8 x^3}{\xi}\right)\text{cm}^{-1}$$

for $x > 0.61$. (5)

TABLE II
ENERGY BANDGAPS AND THRESHOLD ENERGIES FOR DIFFERENT COMPOSITIONS OF $(Al_xGa_{1-x})_{0.52}In_{0.48}P$

Al fraction, x	Minimum energy band gap, E_g [eV]	Ionization threshold energy, E_{th} [eV]
0	1.90	4.05
0.31	2.12	4.35
0.47	2.23	4.57
0.61, 0.64, 0.78, 1	2.24	4.60

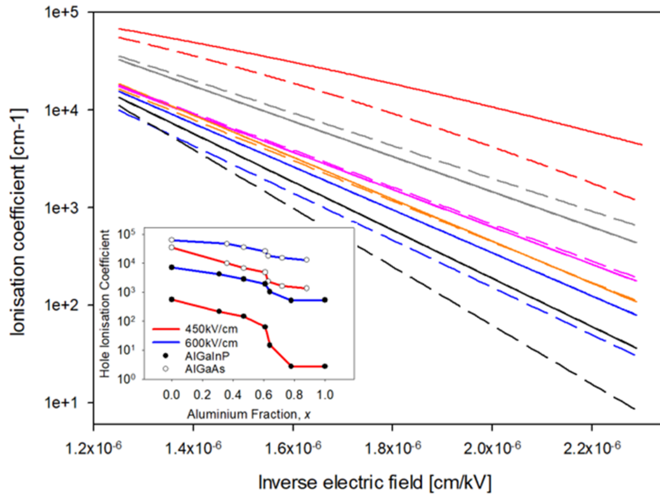

Fig. 4. Electron and hole ionization coefficients for $(Al_xGa_{1-x})_{0.52}In_{0.48}P$ with $x = 0$ (gray), 0.47 (pink), 0.61 (orange), 0.64 (blue), and 1 (black). α is represented by the solid line, and β by the dashed line. Data for $x = 0.78$ and $x = 0.31$ have been omitted for clarity. The coefficients for $x = 0$ and $x = 1$ are those reported by Ghin *et al.* [2] and Ong *et al.* [1], respectively. Data for $Al_{0.8}Ga_{0.2}As$ (red) are included for comparison [19]. Inset shows the change in hole impact ionization coefficient with x for both AlGaInP and AlGaAs.

ionization coefficients depend only on the electric field will predict a slightly lower breakdown voltage and overestimate the excess noise. The coefficients for the ternary endpoints given here therefore differ slightly from those of Ong *et al.* [1] and Ghin *et al.* [2]. These coefficients are approximately related to the enabled ionization coefficients, α^* and β^*, by

$$\frac{1}{\alpha^*(\beta^*)} = \frac{1}{\alpha(\beta)} - \frac{2E_{th}}{\xi} \tag{6}$$

where E_{th} is the ionization threshold energy for the relevant carrier type, and ξ represents electric field in V/cm. α^* and β^* represent the probability of impact ionization events for carriers which have already traversed the dead space.

V. DISCUSSION

From (2)–(5), Fig. 4 shows that both α and β decrease with increasing aluminum fraction. α decreases approximately linearly with increasing x across the full composition range. β however decreases gradually with x up to $x = 0.61$, but then decreases rapidly until $x = 0.78$, after which it remains constant. Interestingly, similar behavior has been observed in AlGaAs, with a sudden decrease in the β when x becomes larger than 0.61 [26]. Although $\beta > \alpha$ in GaInP, the rates

TABLE III
PARAMETERIZED IMPACT IONIZATION COEFFICIENTS OF $Al_xGa_{1-x}As$. COEFFICIENTS ARE EXPRESSED IN THE FORM $A(\exp[-(B/\xi)^C]$, WHERE ξ REPRESENTS ELECTRIC FIELD IN V/CM [27]. THE COEFFICIENTS SHOWN FOR GaAs ARE THOSE OF PLIMMER *et al.* [32]

Al fraction, x		A [x10^5 cm^{-1}]	B [x10^6 cm^{-1}]	C
0 (150kV/cm<F<500kV/cm)	α	1.45	0.50	2.10
	β	1.55	0.55	2.00
0 (500kV/cm<F<1110kV/cm)	α	4.70	1.20	0.90
	β	4.00	1.10	1.00
0.36	α	7.53	1.18	1.45
	β	4.88	0.97	1.76
0.47	α	6.04	1.15	1.51
	β	5.86	1.13	1.63
0.61	α	6.25	1.27	1.50
	β	6.06	1.30	1.49
0.63	α	4.54	1.11	1.63
	β	4.64	1.21	1.68
0.72	α	2.88	0.97	1.80
	β	4.01	1.15	1.82
0.88	α	2.95	1.03	1.68
	β	3.82	1.19	1.78

of decrease mean that β is approximately equal to α for $x = 0.31$–0.61 and $\beta < \alpha$ for higher aluminum compositions. Parameterized impact ionization coefficients for AlGaAs are given in Table III [27]. These coefficients were extracted using a local model, which ignores any dead space effects, from M_e and M_h. The change in β across the composition range of both materials is shown in the inset of Fig. 4 at electric fields of 450 and 600 kV/cm. The reduced excess noise seen in Fig. 3 for the structures with higher aluminum concentrations in both material systems is due to the reduction in β, which results in a smaller β/α ratio.

Using the parameterized ionization coefficients in (2)–(5) and Table III, the breakdown voltages for ideal 1 μm p-i-n structures of AlGaAs and AlGaInP were calculated and are plotted as a function of composition, x, in Fig. 5. It is notable that the breakdown voltages for AlGaInP are the highest of any nonnitride III–V alloy material. V_{bd} initially increases with x in both alloy systems, but changes very little for $x \geq 0.63$ in AlGaAs [26] and remains almost constant for $x \geq 0.64$ in AlGaInP. The breakdown voltages at lower aluminum concentrations are proportional in both alloy systems to the brillouin-zone-averaged indirect energy gap, E_{ind}, as predicted by Allam [28]. The breakdown voltages at higher aluminum compositions deviate from this relationship. E_{ind} is defined as

$$\langle E_{ind} \rangle = \frac{1}{8}[E_\Gamma + 3E_X + 4E_L]. \tag{7}$$

Allam [28] showed that this is related to the breakdown voltage of a 1-μm p-i-n structure in a range of semiconductor materials by

$$V_{bd} = 45.8(\langle E_{ind} \rangle - 1.01). \tag{8}$$

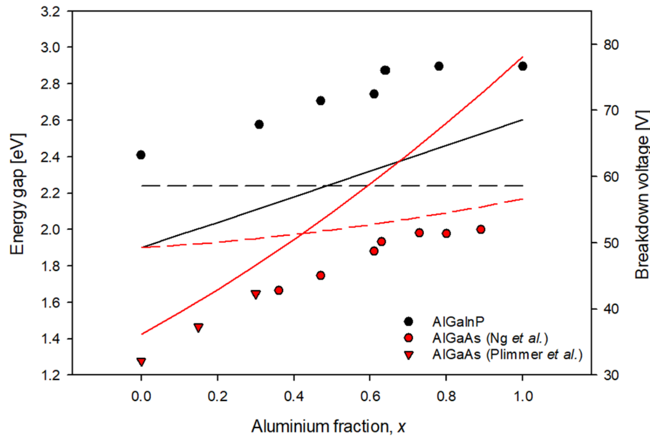

Fig. 5. Breakdown voltages for an ideal 1 μm p-i-n structure with different compositions of $(Al_xGa_{1-x})_{0.52}In_{0.48}P$ (•) and $Al_xGa_{1-x}As$ (○) (right-hand axis). Also shown are the Γ (solid line) and X (dashed line) energy gaps for these material systems (left-hand axis, $Al_xGa_{1-x}As$ in red, $(Al_xGa_{1-x})_{0.52}In_{0.48}P$ in black).

Silicon, which has a very large Γ energy gap, does not obey this relationship and instead uses a modified expression for E_{ind}, which excludes E_Γ due to the fact that carriers from the lower energy satellite valleys are unlikely to gain sufficient energy to scatter into the Γ valley.

The compositions at which V_{bd} saturates are similar in AlGaInP and AlGaAs, and similar to those that exhibit a reduced β/α ratio. This suggests that the same mechanism may responsible for both behaviors. The crossover point between the Γ and X-band minima (when $E_\Gamma > E_X$) occurs at $x = 0.48$ and $x = 0.45$ in AlGaInP and AlGaAs, respectively, [14], [29]. This is significantly lower than the aluminum concentration at which V_{bd} saturates and β rapidly decreases, implying that the crossover is not directly responsible for this change in behavior. After the crossover point, the energy difference between E_Γ and E_X continues to increase in both materials. The saturation of the breakdown voltage implies that there may be a point at which the Γ energy gap becomes sufficiently large that it is no longer involved in the impact ionization process. The $E_\Gamma - E_X$ separation when this happens is significantly larger in the AlGaAs than in AlGaInP, which may be related to the larger electron effective masses in AlGaInP. The reason for the sudden decrease in β seen in high-aluminum composition AlGaInP and AlGaAs is unclear without more detailed modeling of the valence band structure. It is possible that, when E_Γ is much larger than E_X, fewer hole impact ionization events can satisfy the conditions of conservation of energy and momentum.

Hole impact ionization is also likely to be suppressed due to the flattening of the heavy hole band as aluminum content increases [29], which may cause the inter-band scattering rate to increase and prevent holes from accumulating sufficient energy to impact ionize [30]. It is notable that $AlAs_{0.56}Sb_{0.44}$, $Al_{0.85}Ga_{0.15}As_{0.56}Sb_{0.44}$, and $Al_xIn_{1-x}As_ySb_{1-y}$, all of which have recently been reported to have very low β/α ratios [12], [13], [31] are also indirect bandgap semiconductors with the lowest conduction band edge in the X valley.

VI. Conclusion

Electron and hole impact ionization coefficients have been extracted for five different compositions of AlGaInP. It has been observed that the ionization coefficients decrease with increasing aluminum concentration, resulting in an increase in V_{bd} with increasing aluminum content. The β/α ratio also changes from being slightly larger than 1 in GaInP to significantly lower than 1 in AlInP. It has also been observed that β decreases significantly between $x = 0.61$ and $x = 0.78$, but α does not. The breakdown voltage also saturates at the higher aluminum concentrations, in a similar manner to AlGaAs. It is hypothesized that these characteristics are due to the bandgap becoming increasingly indirect as the aluminum concentration increases in both material systems.

References

[1] J. S. L. Ong, J. S. Ng, A. B. Krysa, and J. P. R. David, "Impact ionization coefficients in $Al_{0.52}In_{0.48}P$," *IEEE Electron Device Lett.*, vol. 32, no. 11, pp. 1528–1530, Nov. 2011, doi: 10.1109/LED.2011.2165520.

[2] R. Ghin, J. P. R. David, M. Hopkinson, M. A. Pate, G. J. Rees, and P. N. Robson, "Impact ionization coefficients in GaInPp–i–ndiodes," *Appl. Phys. Lett.*, vol. 70, no. 26, pp. 3567–3569, Jun. 1997, doi: 10.1063/1.119235.

[3] J. P. R. David, M. Hopkinson, and M. A. Pate, "Avalanche breakdown in $(Al_xGa_{1-x})_{0.52}In_{0.48}P$," *Electron. Lett.*, vol. 30, no. 11, pp. 907–909, May 1994.

[4] J. S. Cheong, J. S. L. Ong, J. S. Ng, A. B. Krysa, and J. P. R. David, "$Al_{0.52}In_{0.48}P$ SAM-APD as a blue-green detector," *IEEE J. Sel. Top. Quantum Electron.*, vol. 20, no. 6, pp. 142–146, Nov. 2014, doi: 10.1109/JSTQE.2014.2316601.

[5] L. Qiao *et al.*, "Avalanche noise in $Al_{0.52}In_{0.48}P$ diodes," *IEEE Photon. Technol. Lett.*, vol. 28, no. 4, pp. 481–484, Feb. 15, 2016, doi: 10.1109/LPT.2015.2499545.

[6] J. S. L. Ong, J. S. Ng, A. B. Krysa, and J. P. R. David, "Temperature dependence of avalanche multiplication and breakdown voltage in $Al_{0.52}In_{0.48}P$," *J. Appl. Phys.*, vol. 115, no. 6, Feb. 2014, Art. no. 064507, doi: 10.1063/1.4865743.

[7] R. Ghin, J. P. R. David, M. Hopkinson, M. A. Pate, G. J. Rees, and P. N. Robson, "Impact ionisation and temperature dependence of breakdown in $Ga_{0.52}In_{0.48}P$," in *Proc. Institue Phys. Conf. Ser.*, St. Petersburg, Russia, vol. 8, Sep. 1996, pp. 585–588.

[8] S. Zhao, S. Butera, G. Lioliou, A. B. Krysa, and A. M. Barnett, "High temperature AlInP X-ray spectrometers," *Sci. Rep.*, vol. 9, no. 1, pp. 1–9, Aug. 2019, doi: 10.1038/s41598-019-48394-9.

[9] D. Ji, B. Ercan, G. Benson, A. K. M. Newaz, and S. Chowdhury, "60 A/W high voltage GaN avalanche photodiode demonstrating robust avalanche and high gain up to 525 K," *Appl. Phys. Lett.*, vol. 116, no. 21, May 2020, Art. no. 211102, doi: 10.1063/1.5140005.

[10] A. R. J. Marshall, A. P. Craig, C. J. Reyner, and D. L. Huffaker, "GaAs and AlGaAs APDs with GaSb absorption regions in a separate absorption and multiplication structure using a hetero-lattice interface," *Infr. Phys. Technol.*, vol. 70, pp. 168–170, May 2015, doi: 10.1016/j.infrared.2014.08.014.

[11] W. K. Loke *et al.*, "GaNAsSb/GaAs waveguide photodetector with response up to 1.6 μm grown by molecular beam epitaxy," *Appl. Phys. Lett.*, vol. 93, no. 8, Aug. 2008, Art. no. 081102, doi: 10.1063/1.2976124.

[12] S. Lee *et al.*, "Low noise $Al_{0.85}Ga_{0.15}As_{0.56}Sb_{0.44}$ avalanche photodiodes on InP substrates," *Appl. Phys. Lett.*, vol. 118, no. 8, Feb. 2021, Art. no. 081106, doi: 10.1063/5.0035571.

[13] X. Yi *et al.*, "Extremely low excess noise and high sensitivity $AlAs_{0.56}Sb_{0.44}$ avalanche photodiodes," *Nature Photon.*, vol. 13, no. 10, pp. 683–686, Oct. 2019, doi: 10.1038/s41566-019-0477-4.

[14] J. S. Cheong, A. N. A. P. Baharuddin, J. S. Ng, A. B. Krysa, and J. P. R. David, "Absorption coefficients in AlGaInP lattice-matched to GaAs," *Sol. Energy Mater. Sol. Cells*, vol. 164, pp. 28–31, May 2017, doi: 10.1016/j.solmat.2017.01.042.

[15] D. J. Lockwood, G. Yu, and N. L. Rowell, "Optical phonon frequencies and damping in AlAs, GaP, GaAs, InP, InAs and InSb studied by oblique incidence infrared spectroscopy," *Solid State Commun.*, vol. 136, no. 7, pp. 404–409, Nov. 2005, doi: 10.1016/j.ssc.2005.08.030.

[16] L. G. Meiners, "Temperature dependence of the dielectric constant of InP," *J. Appl. Phys.*, vol. 59, no. 5, pp. 1611–1613, Mar. 1986, doi: 10.1063/1.336472.

[17] B. Monemar, "Determination of band gap and refractive index of AlP from optical absorption," *Solid State Commun.*, vol. 8, no. 16, pp. 1295–1298, Aug. 1970, doi: 10.1016/0038-1098(70)90623-X.

[18] K. A. Bertness, S. R. Kurtz, S. E. Asher, and R. C. Reedy, "AlInP benchmarks for growth of AlGaInP compounds by organometallic vapor-phase epitaxy," *J. Cryst. Growth*, vol. 196, no. 1, pp. 13–22, Jan. 1999, doi: 10.1016/S0022-0248(98)00751-9.

[19] B. K. Ng, J. P. R. David, S. A. Plimmer, M. Hopkinson, R. C. Tozer, and G. J. Rees, "Impact ionization coefficients of $Al_{0.8}Ga_{0.2}As$," *Appl. Phys. Lett.*, vol. 77, no. 26, pp. 4374–4376, Dec. 2000, doi: 10.1063/1.1336556.

[20] R. J. McIntyre, "Multiplication noise in uniform avalanche diodes," *IEEE Trans. Electron Devices*, vol. ED-13, no. 1, pp. 164–168, Jan. 1966, doi: 10.1109/T-ED.1966.15651.

[21] L. Qiao, S. J. Dimler, A. N. A. P. Baharuddin, J. E. Green, and J. P. R. David, "An excess noise measurement system for weak responsivity avalanche photodiodes," *Meas. Sci. Technol.*, vol. 29, no. 6, May 2018, Art. no. 065015, doi: 10.1088/1361-6501/aabc8b.

[22] K. S. Lau *et al.*, "Excess noise measurement in avalanche photodiodes using a transimpedance amplifier front-end," *Meas. Sci. Technol.*, vol. 17, no. 7, pp. 1941–1946, Jun. 2006, doi: 10.1088/0957-0233/17/7/036.

[23] G. E. Stillman and C. M. Wolfe, "Avalanche photodiodes**this work was sponsored by the defense advanced research projects agency and by the department of the air force," in *Semiconductors Semimetals*, vol. 12, R. K. Willardson and A. C. Beer, Eds. Amsterdam, The Netherlands: Elsevier, 1977, pp. 291–393, doi: 10.1016/S0080-8784(08)60150-7.

[24] M. M. Hayat, W. L. Sargeant, and B. E. A. Saleh, "Effect of dead space on gain and noise in Si and GaAs avalanche photodiodes," *IEEE J. Quantum Electron.*, vol. 28, no. 5, pp. 1360–1365, May 1992, doi: 10.1109/3.135278.

[25] J. S. Cheong, M. M. Hayat, X. Zhou, and J. P. R. David, "Relating the experimental ionization coefficients in semiconductors to the nonlocal ionization coefficients," *IEEE Trans. Electron Devices*, vol. 62, no. 6, pp. 1946–1952, Jun. 2015, doi: 10.1109/TED.2015.2422789.

[26] B. K. Ng, J. P. R. David, G. J. Rees, R. C. Tozer, M. Hopkinson, and R. J. Airey, "Avalanche multiplication and breakdown in $Al_xGa_{1-x}As$ (x < 0-9)," *IEEE Trans. Electron Devices*, vol. 49, no. 12, pp. 2349–2351, Dec. 2002.

[27] B. K. Ng, *Impact Ionization in Wide Band Gap Semiconductors: $Al_xGa_{1-x}As$ and 4H-SiC*. Sheffield, U.K.: Univ. Sheffield, 2002.

[28] J. A. J. Allam, "'Universal' dependence of avalanche breakdown on bandstructure: Choosing materials for high-power devices," *Jpn. J. Appl. Phys.*, vol. 36, no. 3S, p. 1529, Mar. 1997, doi: 10.1143/JJAP.36.1529.

[29] S. Adachi, *Properties of Semiconductor Alloys: Group–IV, III–V and II–VI Semiconductors*. Hoboken, NJ, USA: Wiley, 2009.

[30] K. Brennan and K. Hess, "Theory of high-field transport of holes in GaAs and InP," *Phys. Rev. B, Condens. Matter*, vol. 29, no. 10, pp. 5581–5590, May 1984, doi: 10.1103/PhysRevB.29.5581.

[31] A. H. Jones, S. D. March, S. R. Bank, and J. C. Campbell, "Low-noise high-temperature AlInAsSb/GaSb avalanche photodiodes for 2-μm applications," *Nature Photon.*, vol. 14, no. 9, pp. 559–563, Sep. 2020, doi: 10.1038/s41566-020-0637-6.

[32] S. A. Plimmer, J. P. R. David, G. J. Rees, and P. N. Robson, "Ionization coefficients in $Al_xGa_{1-x}As$ (x= 0–0.60)," *Semicond. Sci. Technol.*, vol. 15, no. 7, pp. 692–699, Jun. 2000, doi: 10.1088/0268-1242/15/7/307.